TABLE 3. Summary of the Shortest Overlapping Gains/Amplifications, and Deletions Detected in GCTs

Chromosome region	Shortest overlapping gains/amplifications, and deletions (Mb)			Number of tumors with each SOR	Candidate genes in each SOR
	Start	End	Interval		
1p36.13-p35.3 deletion	19.6	29.1	9.5	19	*RUNX3, LIN28A, WTNT4, ASAP3, RAPIGAP*
3p24.2-p22.1 gain	25.5	41.4	15.9	5	*AZI2, RBMS3, TGFBR2, CTNNB1*
4q21.1-q21.23 deletion	77.0	84.7	7.7	11	*ANXA3*
5q11.2-q13.2 deletion	58.2	68.5	10.3	5	*ERBB2IP*
6q26-qter deletion	162.1	qter	9.0	15	*RPS6KA2, PDCD2, MLL4, SMOC2*
20q13.13-q13.32 gain/amplification	48.4	58.4	10.0	16	*PTPN1, ADNP, BCAS1, AURKA*

UPD, uniparental disomy; SOR, shortest overlapping region.

TABLE 4. Results of Methylation-Specific PCR Analysis of Various Tumor Suppressor Genes and Mutation Analysis of *RUNX3*

Nos.	*RUNX3*	*RASSF1A*	*HOXA9*	*CASP8*	*SCGB3A1*	*SFRP2*	*DCR2*	*RASSF5*	*RASSF2A*	*BLU*	*SFRP5*	*HOXB5*	*p16INK4A*	*p14ARF*	*RIZ1*
1	U	U	U	U	U	U	M	U	NA	U	U	U	U	U	U
2	U	U	U	U	M	U	U	U	U	U	U	U	U	U	U
3	M	M	M	M	M	M	M	U	U	U	U	U	U	U	U
4	U	M	U	U	U	U	U	U	U	U	U	U	U	U	U
5	M	M	M	U	U	U	U	U	U	U	U	U	U	U	U
6	M	M	M	M	M	M	M	M	U	U	U	U	U	U	U
7	M	U	U	U	U	U	U	U	U	U	U	U	U	U	U
8	M	M	M	U	U	M	M	U	M	U	U	U	U	U	U
9	U	U	U	M	U	U	U	U	U	U	U	U	U	U	U
10	M	M	M	M	M	M	M	M	M	U	U	U	U	U	U
11	M	M	M	U	M	U	U	U	M	U	U	M	U	U	U
12	M	M	M	U	M	M	U	U	U	NA	U	NA	U	U	U
13	M	M	M	U	U	U	U	U	U	U	U	U	U	U	U
14	M	M	M	U	M	M	M	U	U	M	U	U	U	U	U
15	M	M	M	M	M	U	M	M	NA	U	U	U	U	U	U
16	M	M	M	M	M	M	U	M	M	U	U	U	U	U	U
17	M	M	M	M	U	U	M	U	U	U	U	U	U	U	U
18	U (NA)	M	M	M	M	M	U	U	U	U	U	U	U	U	U
19	M	U	M	M	M	M	M	M	U	M	U	U	U	U	U
20	M	U	U	M	M	U	U	U	U	U	U	U	U	U	U
21	M	M	M	U	U	U	M	M	M	M	M	U	U	U	U
22	M	M	M	M	U	U	M	U	NA	U	U	U	U	U	U
23	M	M	M	M	U	M	M	M	U	U	U	U	U	U	U
24	M	M	M	U	M	M	M	U	U	U	U	U	U	U	U
25	M	M	M	M	M	M	U	U	NA	U	U	U	U	U	U
26	U (WT)	M	M	U	U	U	U	U	U	U	U	U	U	U	U
27	U (WT)	U	U	U	U	U	U	U	U	U	U	U	U	U	U
28	M	M	M	U	M	M	M	U	U	U	U	U	U	U	U

M, methylated; U, unmethylated; parenthesis after U in a column for *RUNX3* indicates the result of *RUNX3* sequencing; NA, DNA, not available; WT, wild type.

chromosomal heteromorphisms and DNA markers (Deka et al., 1990; Surti et al., 1990; Miura et al., 1999). In addition, we did not find Types II or V tumors in the present series; a previous study of 61 ovarian teratomas reported ~ 40% to be Type II, but could not identify Type V (Deka et al., 1990). Another study reported a low incidence of Type II tumors; only one of 25 teratomas was shown to be Type II (Miura et al., 1999). We could not clarify whether the lack of Type II in the present series was accidental or not, because of the limited number of teratomas included in this study.

Previous comparative genomic hybridization studies identified common chromosomal aberrations, including gains of 1q, 3p, 12p, and 20q, and losses of 1p, 4q, 5q, and 6q (Schneider et al., 2002; Palmer et al., 2007). This study confirmed these findings, and narrowed down the shortest overlapping regions of the gains and losses. Surprisingly, these aberrations were found not only in Type IV tumors but also in Types I and III tumors. 1p−, 4q−, and 20q+ were found in one tumor with segmental UPDs (Type I, Case 3) and another with whole UPD in all chromosomes (Type III, Case 6; Figs. 3B and 4B). The aberrations in Type III are thought to have occurred after the development of whole UPDs, because if 1p− occurred before the whole UPDs, duplication of one 1p− chromosome might have resulted in two homozygous 1p− chromosomes, which was not found in Case 6 (Fig. 4B). The aberrations in Type I are also thought to have occurred after the development of segmental UPDs, because the deletions [1p−, and del(4)(4pter-4q22.1)] did not overlap with the UPD regions, and the allele showing the del(4)(4pter-4q22.1) deletion continuously joined with the allele showing the segmental UPD(4q22.1-4q27), not resulting in a homozygous deletion. Because both tumors (Cases 3 and 6) with segmental or whole UPDs, chromosome aberrations, and many methylated TSGs were diagnosed as yolk sac tumors, and two tumors (Cases 1 and 4) with segmental or whole UPDs, but no aberrations and only one methylated TSG were diagnosed as mature teratomas, genetic and epigenetic alterations may have caused malignant transformation. In Cases 1–6, the methylation patterns of the *SNRPN* and *H19* DMRs indicated a reestablishment of the sex-specific imprint (Fig. 2). These findings point to the malignant transformation of GCT occurring after the reestablishment of imprinting. Thus, we have for the first time found evidence that a benign teratoma could evolve into a malignant tumor, such as a yolk sac tumor. Some investigators have predicted such a malignant evolution based on clinical and pathological findings of ovarian and testicular tumors (Oosterhuis and Looijenga, 2005; Palmer et al., 2007).

With the use of SNP arrays, we narrowed down the shortest overlapping regions of chromosomal gains and losses in GCTs. These included gains and amplifications of 3p24−p22 and 20q13−q13, and losses and UPDs of 1p36−p35, 4q21−q21, 5q11−q13, and 6q26-qter, and the candidate oncogenes and TSGs listed in Table 3. We also found that in most cases, the number of chromosomal aberrations would be distributed in a proportional manner, depending on the number of methylated TSGs (Table. 4). Genetic instability is a common feature in cancer and, in fact, mutations in genes involved in processes like DNA repair, chromosomal segregation, checkpoint control, and centrosome duplication are oncogenic (Lengauer et al., 1998; Negrini et al., 2010). Because many TSGs are specialized in controlling these processes, down-regulation of TSGs by promoter methylation may contribute to genetic instability.

The most common region for deletion was 1p36.13-p35.3, where two important genes, *RUNX3* and *LIN28A*, are located. The Runt-related transcription factors (RUNX) are a family of evolutionarily conserved metazoan proteins, which share the highly homologous N-terminal Runt domain, a DNA-binding domain, and a heterodimerization region of about 120 amino acids. Functional inactivation of *RUNX3* is frequent in solid tumors of diverse origins (Goel et al., 2004; Li et al., 2004; Xiao and Liu, 2004). In most cases, inactivation is caused by silencing of the gene by promoter hypermethylation. In addition, missense and truncating mutations were also reported in the highly conserved Runt domain although at a much lower incidence than promoter methylation (Kim et al., 2005). Deletion of 1p36-p35 was found in 19 of 28 tumor samples, and *RUNX3* was methylated in 16 of the 19 tumors (Table 4; Furukawa et al., 2009). Sequencing showed no mutation in the Runt domain in two of the three tumors with 1p36 deletion and unmethylated *RUNX3*. Thus, the main cause of inactivation of this gene seemed to be promoter hypermethylation. The promoter of *RUNX3* is methylated in normal stem cells, but the significance of *RUNX3* methylation remains elusive (Blyth et al., 2005).

LIN28A, which resides at 1p36.1 and was found to be overexpressed in human ovarian GCTs by immunohistochemistry (Xue et al., 2011), is another candidate gene, although the finding of 1p36 loss is contradictory to *LIN28*A overexpression, which is supposed to be the activity of oncogenes. Some candidate genes such as *RAP1-GAP*, *ANXA3*, and *AURKA*, which reside at 1p36, 4q21, and 20q13, respectively, are thought to contribute to germ cell tumorigenesis.

In conclusion, we present here an example of malignant transformation of a benign teratoma to

a yolk sac tumor. We also narrowed down the shortest overlapping regions for gains/amplifications and losses/UPDs, which were previously reported in childhood and adult GCTs. Further analysis of the candidate genes in the regions might allow us to unveil the tumorigenesis of GCT.

ACKNOWLEDGMENTS

The authors express our gratitude to the patients and physicians who supplied samples and clinical data for this study.

REFERENCES

Bussey KJ, Lawce HJ, Himoe E, Shu XO, Heerema NA, Perlman EJ, Olson SB, Magenis RE. 2001. *SNRPN* methylation patterns in germ cell tumors as a reflection of primordial germ cell development. Genes Chromosomes Cancer 32:342–352.

Blyth K, Cameron ER, Neil JC. 2005. The *RUNX* genes: gain or loss of function in cancer. Nat Rev Cancer 5:376–387.

Deka R, Chakravarti A, Surti U, Hauselman E, Reefer J, Majumder PP, Ferrell RE. 1990. Genetics and biology of human ovarian teratomas. II. Molecular analysis of origin of nondisjunction and gene-centromere mapping of chromosome I markers. Am J Hum Genet 47:644–655.

Furukawa S, Haruta M, Arai Y, Honda S, Ohshima J, Sugawara W, Kageyama Y, Higashi Y, Nishida K, Tsunematsu Y, Nakadate H, Ishii M, Kaneko Y. 2009. Yolk sac tumor but not seminoma or teratoma is associated with abnormal epigenetic reprogramming pathway and shows frequent hypermethylation of various tumor suppressor genes. Cancer Sci 100:698–708.

Gabory A, Ripoche MA, Yoshimizu T, Dandolo L. 2006. The *H19* gene: regulation and function of a non-coding RNA. Cytogenet Genome Res 113:188–193.

Goel A, Arnold CN, Tassone P, Chang DK, Niedzwiecki D, Dowell JM, Wasserman L, Compton C, Mayer RJ, Bertagnolli MM, Boland CR. 2004. Epigenetic inactivation of *RUNX3* in microsatellite unstable sporadic colon cancers. Int J Cancer 112:754–759.

Haruta M, Arai Y, Sugawara W, Watanabe N, Honda S, Ohshima J, Soejima H, Nakadate H, Okita H, Hata J, Fukuzawa M, Kaneko Y. 2008. Duplication of paternal *IGF2* or loss of maternal *IGF2* imprinting occurs in half of Wilms tumors with various structural *WT1* abnormalities. Genes Chromosomes Cancer 47:712–727.

Honda S, Haruta M, Sugawara W, Sasaki F, Ohira M, Matsunaga T, Yamaoka H, Horie H, Ohnuma N, Nakagawara A, Hiyama E, Todo S, Kaneko Y. 2008. The methylation status of *RASSF1A* promoter predicts responsiveness to chemotherapy and eventual cure in hepatoblastoma patients. Int J Cancer 123:1117–1125.

Horsthemke B, Buiting K. 2006. Imprinting defects on human chromosome 15. Cytogenet Genome Res 113:292–299.

Japanese Pathological Society. 1999. Germ cell tumors and sex cord/stromal tumors in childhood. Committee on histological classification of childhood tumors. Tokyo: Kanahara Shuppan.

Kim WJ, Kim EJ, Jeong P, Quan C, Kim J, Li QL, Yang JO, Ito Y, Bae SC. 2005. *RUNX3* inactivation by point mutations and aberrant DNA methylation in bladder tumors. Cancer Res 65:9347–9354.

Kobayashi H, Sato A, Otsu E, Hiura H, Tomatsu C, Utsunomiya T, Sasaki H, Yaegashi N, Arima T. 2007. Aberrant DNA methylation of imprinted loci in sperm from oligospermic patients. Hum Mol Genet 16:2542–2551.

Lengauer C, Kinzler KW, Vogelstein B. 1998. Genetic instabilities in human cancers. Nature 396:643–649.

Li QL, Kim HR, Kim WJ, Choi JK, Lee YH, Kim HM, Li LS, Kim H, Chang J, Ito Y, Youl Lee K, Bae SC. 2004. Transcriptional silencing of the *RUNX3* gene by CpG hypermethylation is associated with lung cancer. Biochem Biophys Res Commun 314:223–228.

Lind GE, Skotheim RI, Fraga MF, Abeler VM, Esteller M, Lothe RA. 2006. Novel epigenetically deregulated genes in testicular cancer include homeobox genes and SCGB3A1 (HIN-1). J Pathol 210:441–449.

Miura K, Obama M, Yun K, Masuzaki H, Ikeda Y, Yoshimura S, Akashi T, Niikawa N, Ishimaru T, Jinno Y. 1999. Methylation imprinting of *H19* and *SNRPN* genes in human benign ovarian teratomas. Am J Hum Genet 65:1359–1367.

Mostert M, Rosenberg C, Stoop H, Schuyer M, Timmer A, Oosterhuis W, Looijenga L. 2000. Comparative genomic and in situ hybridization of germ cell tumors of the infantile testis. Lab Invest 80:1055–1064.

Nannya Y, Sanada S, Nakazaki K, Hosoya N, Wang L, Hangaishi A, Kurokawa M, Chiba S, Bailey DK, Kennedy GC, Ogawa S. 2005. A robust algorithm for copy number detection using high density oligonucleotide single nucleotide polymorphism genotyping arrays. Cancer Res 65:6071–6079.

Negrini S, Gorgoulis VG, Halazonetis TD. 2010. Genomic instability—an evolving hallmark of cancer. Nat Rev Mol Cell Biol 11:220–228.

Oosterhuis JW, Looijenga LH. 2005. Testicular germ-cell tumours in a broader perspective. Nat Rev Cancer 5:210–222.

Palmer RD, Foster NA, Vowler SL, Roberts I, Thornton CM, Hale JP, Schneider DT, Nicholson JC, Coleman N. 2007. Malignant germ cell tumours of childhood: new associations of genomic imbalance. Br J Cancer 96:667–676.

Perlman EJ, Hu J, Ho D, Cushing B, Lauer S, Castleberry RP. 2000. Genetic analysis of childhood endodermal sinus tumors by comparative genomic hybridization. J Pediatr Hematol Oncol 22:100–105.

Rickert CH, Simon R, Bergmann M, Dockhorn-Dworniczak B, Paulus W. 2000. Comparative genomic hybridization in pineal germ cell tumors. J Neuropathol Exp Neurol 59:815–821.

Riopel MA, Spellerberg A, Griffin CA, Perlman EJ. 1998. Genetic analysis of ovarian germ cell tumors by comparative genomic hybridization. Cancer Res 58:3105–3110.

Schneider DT, Schuster AE, Fritsch MK, Hu J, Olson T, Lauer S, Göbel U, Perlman EJ. 2001. Multipoint imprinting analysis indicates a common precursor cell for gonadal and nongonadal pediatric germ cell tumors. Cancer Res 61: 7268–7276.

Schneider DT, Schuster AE, Fritsch MK, Calaminus G, Göbel U, Harms D, Lauer S, Olson T, Perlman EJ. 2002. Genetic analysis of mediastinal nonseminomatous germ cell tumors in children and adolescents. Genes Chromosomes Cancer 34: 115–125.

Schneider DT, Zahn S, Sievers S, Alemazkour K, Reifenberger G, Wiestler OD, Calaminus G, Göbel U, Perlman EJ. 2006. Molecular genetic analysis of central nervous system germ cell tumors with comparative genomic hybridization. Mod Pathol 19: 864–873.

Sievers S, Alemazkour K, Zahn S, Perlman EJ, Gillis AJ, Looijenga LH, Göbel U, Schneider DT. 2005. *IGF2/H19* imprinting analysis of human germ cell tumors (GCTs) using the methylation-sensitive single-nucleotide primer extension method reflects the origin of GCTs in different stages of primordial germ cell development. Genes Chromosomes Cancer 44: 256–264.

Surti U, Hoffner L, Chakravarti A, Ferrell RE. 1990. Genetic and biology of human ovarian teratomas. I. Cytogenetic analysis and mechanism of origin. Am J Hum Genet 47:635–643.

van Echten J, Timmer A, van der Veen AY, Molenaar WM, de Jong B. 2002. Infantile and adult testicular germ cell tumors. A different pathogenesis?Cancer Genet Cytogenet 135:57–62.

Watanabe N, Haruta M, Soejima H, Fukushi D, Yokomori K, Nakadate H, Okita H, Hata JI, Fukuzawa M, Kaneko Y. 2007. Duplication of the paternal *IGF2* allele in trisomy 11 and elevated expression levels of *IGF2* mRNA in congenital mesoblastic nephroma of the cellular or mixed type. Genes Chromosomes Cancer 46:929–935.

Woodward PJ, Heidenreich A, Looijenga LHJ, Oosterhuis JW, McLeod DG, Møller H, Manivel JC, Mostofi FK, Hailemariam S, Parkinson MC, Grigor K, True L, Jacobsen GK, Oliver TD, Talerman A, Kaplan GW, Ulbright TM, Sesterhenn IA, Rushton HG, Michael H, Reuter VE. 2004.Germ cell tumors. In: Eble JN, Suter G, Epstein JI, Sesterhenn IA, editors. World Health Organization classification of tumours. Pathology and genetics of tumours of the urinary system and male genital organs.Lyon:IARC Press. p. 221–249.

Xiao WH, Liu WW. 2004. Hemizygous deletion and hypermethylation of RUNX3 gene in hepatocellular carcinoma. World J Gastroenterol 10:376–380.

Xue D, Peng Y, Wang F, Allan R W, Cao D. 2011. RNA-binding protein LIN28 is a sensitive marker of ovarian primitive germ cell tumours. Histopathology 59:452–459.

Yamamoto Y, Nannya Y, Kato M, Sanada M, Levine RL, Kawamata N, Hangaishi A, Kurokawa M, Chiba S, Gilliland DG, Koeffler HP, Ogawa S. 2007. Highly sensitive method for genome wide detection of allelic composition in nonpaired, primary specimens by use of Affymetrix single-nucleotide-polymorphism genotyping microarrays. Am J Hum Genet 81:114–126.

Young JL Jr., Ries LG, Silverberg E, Horm JW, Miller RW. 1986. Cancer incidence, survival, and mortality for children younger than age 15 years. Cancer 58:598–602.

Pediatr Transplantation 2013: 17: E29–E32

Pediatric Transplantation
DOI: 10.1111/j.1399-3046.2012.01762.x

Successful bone marrow transplantation with reduced intensity conditioning in a patient with delayed-onset adenosine deaminase deficiency

Kanegane H, Taneichi H, Nomura K, Wada T, Yachie A, Imai K, Ariga T, Santisteban I, Hershfield MS, Miyawaki T. Successful bone marrow transplantation with reduced intensity conditioning in a patient with delayed-onset adenosine deaminase deficiency.

Abstract: In this case report, we describe successful BMT with RIC in a patient with delayed-onset ADA deficiency. A three-yr-old Japanese boy was diagnosed with delayed-onset ADA deficiency because of recurrent bronchitis, bronchiectasia, and lymphopenia. In addition, autoimmune thyroiditis and neutropenia were present. At four yr of age, he underwent BMT with a RIC regimen, including busulfan and fludarabine, from an HLA-identical healthy sister. Engraftment after BMT was uneventful without GVHD. Decreased ADA levels in blood immediately increased following BMT, and the patient was disease-free 13 months after BMT. These results suggest that BMT with RIC may sufficiently restore immune regulation in delayed-onset ADA deficiency. A longer follow-up period is needed to confirm these observations.

Hirokazu Kanegane[1], Hiromichi Taneichi[1], Keiko Nomura[1], Taizo Wada[2], Akihiro Yachie[2], Kohsuke Imai[3], Tadashi Ariga[4], Ines Santisteban[5], Michael S. Hershfield[5] and Toshio Miyawaki[1]

[1]Department of Pediatrics, Graduate School of Medicine and Pharmaceutical Sciences, University of Toyama, Toyama, Japan, [2]Department of Pediatrics, School of Medicine, Institute of Medical, Pharmaceutical and Health Sciences, Kanazawa University, Kanazawa, Japan, [3]Department of Community Pediatrics, Perinatal and Maternal Medicine, Graduate School of Medicine, Tokyo Medical and Dental University, Tokyo, Japan, [4]Department of Pediatrics, Hokkaido University Graduate School of Medicine, Sapporo, Japan, [5]Department of Medicine and Biochemistry, Duke University Medical Center, Durham, NC, USA

Key words: adenosine deaminase deficiency – delayed-onset – bone marrow transplantation – *reduced intensity conditioning*

Hirokazu Kanegane, Department of Pediatrics, Graduate School of Medicine and Pharmaceutical Sciences, University of Toyama, 2630 Sugitani, Toyama, Toyama 930-0194, Japan
Tel.: 81 76 434 7313
Fax: 81 76 434 5029
E-mail: kanegane@med.u-toyama.ac.jp

Accepted for publication 29 May 2012

ADA deficiency is a disorder of purine metabolism, which results in abnormalities in immune system development and function (1, 2). A majority of ADA deficiency cases indicate SCID during infancy; however, approximately 15% of ADA-deficient patients present with symptoms after infancy, which is referred to as a delayed- or late-onset type. Patients with delayed-onset ADA deficiency exhibit variable clinical symptoms, including bacterial infections and autoimmune manifestations. Allogeneic hematopoietic stem cell transplantation has long been a gold standard for the treatment of ADA-SCID; however, two other second-line options are available for ADA-SCID: Enzyme replacement therapy with PEG-ADA and hematopoietic stem cell gene therapy (3). The treatment of choice for delayed-onset ADA deficiency remains unclear because of

Abbreviation: ADA, adenosine deaminase; BMT, bone marrow transplantation; dAXP, deoxyadenosine nucleotides; GVHD, graft-versus-host disease; HLA, human leukocyte antigen; PEG, polyethylene-glycosylated; PEG-ADA, polyethylene-glycosylated bovine ADA; RIC, reduced intensity conditioning; SCID, severe combined immunodeficiency; sjKRECs, signal joint κ-deleting recombination excision circles; TCR, T-cell receptor; TRECs, T-cell receptor excision circles.

the clinical variety. We report on a four-yr-old Japanese boy with delayed-onset ADA deficiency who underwent BMT with RIC from a HLA-identical healthy sister.

Case report

The patient was previously described (4). He is a boy who was admitted to our hospital at three yr of age for the investigation of recurrent infectious episodes. The patient did not have a neurological deficit. Laboratory data revealed neutropenia (600/μL), lymphocytopenia (580/μL), elevated C-reactive protein (7.43 mg/dL; normal, <0.29 mg/dL) and elevated thyroid-stimulating hormone (133 μIU/mL; normal, 0.35–3.73 μIU/mL). Anti-neutrophil, anti-nuclear, anti-thyroglobulin, and anti-thyroid peroxidase antibodies were positive, indicating that autoimmune neutropenia and thyroiditis were present. Chest computed tomography disclosed bronchiectasia. An immunological study indicated hypergammaglobulinemia, but a low percentage of IgG2 subclass antibodies (5.41%; normal, 20–30%) was obtained. The lymphocyte subsets revealed an expansion of the $CD45RO^+$ (memory) populations of $CD4^+$ and $CD8^+$ T cells (74.8% and 39.6%, respectively) and an extremely reduced number of $CD20^+$ B cells (0.2%). TRECs and signal joint κ-deleting recombination excision circles (sjKRECs) were quantified by real-time PCR as previously described (5, 6) and were undetectable. Flow cytometry analysis of the TCR Vβ repertoire was performed as described previously (7), and the analysis revealed an extremely skewed pattern in $CD8^+$ T cells but not in $CD4^+$ T cells (Fig. 1). Therefore, the patient was clinically presumed to have a combined immunodeficiency with autoimmune manifestations, possibly indicating delayed-onset ADA deficiency. The ADA and dAXP levels in whole blood were measured using the extracts of dried blood spots (8). ADA was found to be decreased (1.0 μmol/h/mg protein; normal, 26.4 $\pm$ 10.0 μmol/h/mg protein), and %dAXP increased to 10.8% (normal $<$ 1%). These data led to a diagnosis of ADA deficiency. An analysis of the *ADA* gene disclosed that the patient had compound heterozygous mutations (R156C and V177M). This genotype is compatible with delayed-onset ADA deficiency (9, 10).

The patient was treated with intravenous immunoglobulin replacement therapy, and oral administration of trimethoprim–sulfamethoxazole, acyclovir, and levothyroxine. He was nearly free from infections; however, his serum immunoglobulin levels gradually decreased. We identified his healthy sister as an HLA-identical donor with no mutation in the *ADA* gene. At the age of four yr, the patient underwent BMT. He was treated with conditioning, which consisted of fludarabine (30 mg/m^2/day $\times$ six days, days -7 to -2) and intravenous reduced dose busulfan (4.4 mg/kg/day $\times$ two days, days -3 to -2). The patient received 6.9×10^8 nucleated cells/kg containing 3.1×10^6 $CD34^+$ cells/kg to achieve rapid engraftment. Cyclosporin A was used as GVHD prophylaxis. The post-transplant clinical course was without major complications, and no signs of acute GVHD were observed. The patient did not receive blood transfusion, and engraftments of neutrophils ($>500/\mu$L) and thrombocytes ($>50\,000/\mu$L) were achieved at days 18 and 35, respectively. Cyclosporin A was stopped at day 46. The patient is currently well and has not suffered from any major infectious episodes. The patient received levothyroxine at a low dose; however, anti-thyroglobulin and anti-thyroid peroxidase antibodies became negative. The patient went off immunoglobulin replacement therapy 11 months after BMT.

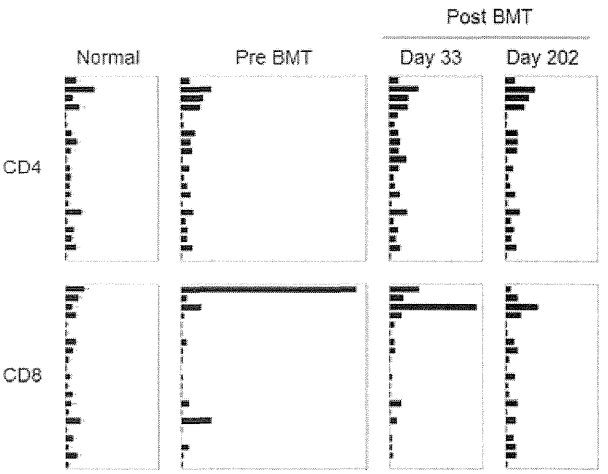

Fig. 1. TCR Vβ repertoire in the $CD4^+$ and $CD8^+$ T cells that were analyzed pre-BMT and post-BMT on days 23 and 202. The TCR Vβ repertoire was analyzed by flow cytometry as previously described (7).

Donor engraftment was evaluated by PCR amplification of the microsatellite marker D8S1179. Donor engraftment in granulocytes and B cells was observed at days 33 and 83, respectively. Complete donor engraftment in whole cells was achieved at day 323 (Table 1). Consistent with high chimerism, the patient exhibited a rapid increase in ADA activity and fast metabolic detoxification by day 83 (Table 2). In addition, immunological studies indicated rapid reconstitution of the lymphocyte subpopulation, and B cells increased to a normal level (305/μL;

Table 1. Engraftment of donor cells in different cell lineages

	Donor cell engraftment (%)				
Post-BMT	Whole blood	Lymphocytes	T cells	B cells	Granulocytes
Day 12	8.5	NA	14.2	NA	0
Day 33	50.7	33.0	NA	NA	100.0
Day 83	80.5	NA	16.5	100.0	100.0
Day 323	>95.0	NA	>95.0	100.0	100.0

NA, not applicable.
Analyses of donor cell engraftment according to a chimerism assay in the peripheral blood of the patient at different time points after BMT.

Table 2. ADA activity in the whole blood of the patient

Samples	ADA (μmol/h/mg protein)	%dAXP
Pre-BMT	1.0	10.8
Day 25	8.7	1.1
Day 83	33.7	0.0
ADA-SCID	0.38 ± 0.5	50.3 ± 18.0
Normal levels	26.4 ± 10.0	<1

The data are from the analyses of the extracts of dried blood spots.

age-matched control, 278–922/μL) at day 97 (Fig. 2). TREC and sjKREC levels reached normal levels at days 83 and 202, respectively (Table 3). The $CD45RO^+$ (memory) populations of $CD4^+$ T cells decreased to a normal range (21.9 ± 4.4%) soon after BMT. Sequential TCR Vβ repertoire analyses revealed that the polyclonal patterns in $CD4^+$ T cells were consistent after BMT, and the extremely skewed pattern in $CD8^+$ T cells had improved by day 202 (Fig. 1).

Discussion

ADA-SCID is a complex immune and metabolic disorder that results from a lack of ADA, which is a key enzyme in purine metabolism. Patients with ADA-SCID have recurrent and severe infections, growth retardation and organ failure. The first treatment of choice is BMT from an HLA-identical sibling donor, if available, followed by treatments for other forms of SCID. Second-line treatments for patients without an HLA-identical donor include enzyme replacement therapy with PEG-ADA, matched unrelated donor hematopoietic stem cell transplantation and hematopoietic stem cell gene therapy (3). Although the treatment strategy for ADA-SCID is well-established, treatment for delayed-onset ADA deficiency is not standardized because of the various clinical conditions. In this study, an HLA-identical healthy sibling donor was available, and we selected BMT from this donor to treat the patient. In cases of ADA-SCID, BMT from an HLA-identical donor is undertaken without a preparative conditioning regimen. The largest series of SCID patients from the European SCETIDE database included 475 patients (11). Of these patients, 51 patients with ADA-SCID had a three-yr survival rate of 81% for HLA-matched transplantation, but 29% for HLA-mismatched transplantation. A recently published cohort study demonstrated that hematopoietic stem cell transplantation in patients with SCID, including ADA deficiency, resulted in engraftment and long-term survival for the majority of patients with or without conditioning (12). However, transplantation without conditioning may result in partial donor engraftment, causing reduced immune reconstitution. Alternatively, hematopoietic stem cell gene therapy is effective for ADA-SCID patients who lack an HLA-identical sibling donor (13). Autologous $CD34^+$ bone marrow cells were transduced with a retroviral vector containing the ADA gene and infused into 10 patients with ADA-SCID after non-myeloablative conditioning. However, two patients have required enzyme replacement after gene therapy (14). ADA gene therapy has been performed in total 31 patients in Italy, the United Kingdom, and the United States. Twenty-one patients have been successful, whereas 10 patients have received enzyme replacement therapy (15). Recently, Cancrini et al. (16) described two ADA-SCID patients from the same family who both underwent BMT. One patient underwent BMT without conditioning, whereas

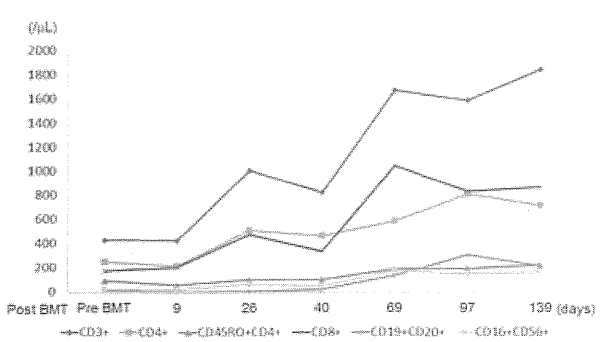

Fig. 2. Kinetics of the lymphocyte subpopulations in the patient.

Table 3. TREC and sjKREC levels as measured by quantitative PCR in the peripheral blood at different time points

	Post-BMT Day 25	Day 83	Day 202	Normal values
TRECs	0	8.1×10^3	1.9×10^3	$3.5 \pm 2.8 \times 10^3$
sjKRECs	0	2.8×10^2	6.4×10^3	$4.8 \pm 0.6 \times 10^3$
RNaseP	4.5×10^4	1.6×10^5	2.0×10^5	

All of the units are copies/μg DNA. The RNaseP gene was amplified as an internal control. The normal values indicate the copy numbers of the age-matched controls (2–6 yr of age).

the other patient was administered a RIC regimen (busulfan and fludarabine) following the failure of cord blood transplantation. Engraftment and immune reconstitution were compared in these patients. The patient who received conditioning exhibited stable mixed chimerism in all of the cell lineages, whereas the patient who underwent BMT without conditioning exhibited slow immune reconstitution, especially in B and myeloid cells. This observation indicated that the use of conditioning resulted in faster immunologic and metabolic reconstitution. In these patients, the immune reconstitution of B and myeloid cells was slower than that of T and NK cells. Interestingly, the reconstitution of myeloid and B cells appeared earlier than that of T cells in our patient. The patient with delayed-onset ADA deficiency had a substantial number of T cells but no B cells before BMT, and the generation of new T cells may take longer than B cells.

Patients with delayed-onset ADA deficiency often have chronic pulmonary insufficiency and autoimmune phenomena, including cytopenia and anti-thyroid antibodies, as observed in our patient. Patients with a delayed- or late-onset type may survive undiagnosed in the first decade of life or beyond; however, the longer the disease goes undiagnosed, the more the immune function deteriorates. The serum immunoglobulin levels of our patient gradually decreased from the point of diagnosis. Our patient had a substantial number of T cells; however, TRECs were undetectable in his peripheral blood. Therefore, we decided that the patient would receive BMT preceded by a RIC regimen, including busulfan and fludarabine. The use of RIC in BMT from an HLA-identical donor in this patient resulted in rapid and complete immune and metabolic reconstitution, and there was no treatment-related toxicity. However, a longer follow-up period is required to confirm these observations. If patients have an HLA-identical sibling donor, BMT with a RIC regimen may be the treatment of choice in patients with delayed-onset ADA deficiency.

Acknowledgments

We would like to thank Mr. Hitoshi Moriuchi, Ms. Chikako Sakai, and Ms. Junko Michino for their technical assistance, and Dr. Bobby Gaspar for critical discussions. We are also grateful to Drs. Hideyuki Nakaoka, Takuya Wada, Akiko Sugiyama, Xi Yang, Shunichiro Takezaki, Masafumi Yamada, Osamu Ohara, Shigeaki Nonoyama, and Chikako Kamae for their clinical and experimental support.

Source of funding

This work was supported by a Grant-in-Aid for Scientific Research from the Ministry of Education, Culture, Sports, Science and Technology of Japan and a grant for Research on Intractable Disease from the Ministry of Health, Labor and Welfare of Japan.

References

1. Hershfield MS. Combined immune deficiency due to purine enzyme defects. In: Stiehm ER, Ochs HD, Winkelstein JA, eds. Immunologic Disorders in Infants and Children. Philadelphia, PA: WB Saunders, 2004: pp. 480–504.
2. Hirshhorn R, Candotti F. Immunodeficiency disease due to defects of purine metabolism. In: Ochs HD, Smith CIE, Puck JM, eds. Primary Immunodeficiency Diseases: A Molecular and Genetic Approach. New York, NY: Oxford University Press, 2007: pp. 169–196.
3. Gaspar HB, Aiuti A, Porta F, Candotti F, Hershfield MS, Notarangelo LD. How I treat ADA deficiency. Blood 2009: 114: 3524–3532.
4. Nakaoka H, Kanegane H, Taneichi H, et al. Delayed onset adenosine deaminase deficiency associated with acute disseminated encephalomyelitis. Int J Hematol 2012: 95: 692–696.
5. Morinishi Y, Imai K, Nakagawa N, et al. Identification of severe combined immunodeficiency by T-cell receptor excision circles quantification using neonatal Guthrie cards. J Pediatr 2009: 155: 829–833.
6. Nakagawa N, Imai K, Kanegane H, et al. Quantification of κ-deleting recombination excision circles in Guthrie cards for the identification of early B-cell maturation defects. J Allergy Clin Immunol 2011: 128: 223–225.e2.
7. Toga A, Wada T, Sakakibara Y, et al. Clinical significance of cloned expansion and CD5 down-regulation in Epstein–Barr virus (EBV)-infected CD8+ T lymphocytes in EBV-associated hemophagocytic lymphohistiocytosis. J Infect Dis 2010: 201: 1923–1932.
8. Arrendondo-Vega FX, Santisteban I, Richard E, et al. Adenosine deaminase deficiency with mosaicism for a "second-site suppressor" of a splicing mutation: Decline in revertant T lymphocytes during enzyme replacement therapy. Blood 2002: 99: 1005–1013.
9. Arrendondo-Vega FX, Santisteban I, Daniels S, Toutain S, Hershfield MS. Adenosine deaminase deficiency: Genotype-phenotype correlations based expressed activity of 29 mutant alleles. Am J Hum Genet 1998: 63: 1049–1059.
10. Hershfield MS. Genotype is an important determinant of phenotype in adenosine deaminase deficiency. Curr Opin Immunol 2003: 15: 571–577.
11. Antoine C, Muller S, Cant A, et al. Long-term survival and transplantation of haematopoietic stem cells for immunodeficiencies: Report of the European experience 1968–99. Lancet 2003: 361: 553–560.
12. Patel NC, Chinen J, Rosenblatt HM, et al. Outcomes of patients with severe combined immunodeficiency treated with hematopoietic stem cell transplantation with and without preconditioning. J Allergy Clin Immunol 2009: 124: 1062–1069.
13. Aiuti A, Cattaneo F, Galimberti S, et al. Gene therapy for immunodeficiency due to adenosine deaminase deficiency. N Engl J Med 2009: 360: 447–458.
14. Aiuti A, Roncarrolo MG. Ten years of gene therapy for primary immunodeficiencies. Hematology Am Soc Hematol Educ Program 2009: 682–689.
15. Fischer A, Hacein-Bey-Abina S, Cavazzana-Calvo M. Gene therapy for primary adaptive immune deficiencies. J Allergy Clin Immunol 2011: 127: 1356–1359.
16. Cancrini C, Ferrua F, Scarselli A, et al. Role of reduced intensity conditioning in T-cell and B-cell immune reconstitution after HLA-identical bone marrow transplantation in ADA-SCID. Haematologica 2010: 95: 1778–1782.

Eur J Pediatr (2013) 172:1263–1265
DOI 10.1007/s00431-013-2034-3

SHORT COMMUNICATION

Rapid progression to pulmonary arterial hypertension crisis associated with mixed connective tissue disease in an 11-year-old girl

Yuka Okura · Shunichiro Takezaki · Yasuhiro Yamazaki · Masafumi Yamada · Ichiro Kobayashi · Tadashi Ariga

Received: 17 March 2013 / Accepted: 6 May 2013 / Published online: 18 May 2013

Abstract Mixed connective tissue disease (MCTD) is rare in pediatric rheumatic diseases. Pulmonary arterial hypertension (PAH) associated with MCTD usually progresses gradually and is difficult to note at the asymptomatic phase. We report a 11-year-old girl with MCTD complicated with rapidly progressive PAH. Although PAH was not detected by echocardiogram or chest CT scan at the initial examination, it became clear in 1 year and suddenly came to cardiac arrest during an invasive procedure. She was successfully treated with extracorporeal assist and both vasodilative and immunosuppressive medication. A combination of echocardiogram and plasma BNP levels could be a useful marker for the follow-up of such cases. PAH could develop early in the course of pediatric MCTD and needs attention to unexpected acute exacerbation, especially under emotional stress.

Keywords Mixed connective tissue disease · Pulmonary arterial hypertension · Pulmonary arterial hypertension crisis · Pulmonary function test · B-type natriuretic peptide

Introduction

Mixed connective tissue disease (MCTD) is characterized by Raynaud phenomenon (RP) or swollen hands, overlapping clinical features of systemic lupus erythematosus (SLE), systemic sclerosis (SSc), and polymyositis/dermatomyositis in conjunction with the presence of anti-ribonucleoprotein (RNP) antibodies [3]. MCTD is rare in children and constitutes 0.6 % of pediatric rheumatic diseases [5]. The poor prognosis is associated with the presence of interstitial lung diseases or pulmonary arterial hypertension (PAH). PAH is more severe in adult MCTD; however, it tends to progresses gradually [1]. Here, we report an 11-year-old girl with rapidly progressive PAH associated with MCTD.

Y. Okura (✉) · S. Takezaki · Y. Yamazaki · M. Yamada · I. Kobayashi · T. Ariga
Department of Pediatrics, Hokkaido University Graduate School of Medicine, North 15 West 7, Kita-ku, Sapporo 060-8638,, Japan
e-mail: okura@med.hokudai.ac.jp

Case report

A 10-year-old Japanese girl was referred to our hospital because of RP since the age of 9 years. She also showed swollen fingers. Laboratory findings were as follows: white blood cell count 4.1× 10^9/L with normal differentiation, hemoglobin 118 g/L, platelet count 216×10^9 /L, erythrocyte sedimentation rate 32 mm/h, C-reactive protein<0.2 mg/L (normal range, <3.9), C3 1.00 g/L (normal range, 0.86–1.60), C4 0.17 g/L (normal range, 0.17–0.45), CH50 59.2 U/ mL (normal range, 31.5–48.4), immunoglobulin (Ig) G 19.23 g/L (normal range, 8.70-17.00), antinuclear antibody titer>1:1,280 (normal range, 0–1:20), and anti-RNP antibodies, autoantibodies related to MCTD, 152.4 INDEX (normal range, <12.9). SLE-specific autoantibodies such as anti-double-stranded DNA and anti-Smith antibodies or SSc-specific antibodies such as anti-topoisomerase antibodies were all negative. Pulmonary function test (PFT) showed slightly decreased percentage of diffusing capacity of carbon monoxide (%DLCO, 65.6 %) and normal % vital capacity (%VC, 82 %). There was no evidence of PAH or interstitial pneumonia (IP) on either echocardiographic study or chest computed tomography (CT) scan. Plasma B-type natriuretic peptide (BNP) level was 20.5 pg/mL (normal

range, <18.4). The chest X-ray showed normal cardiothoracic ratio (CTR) 50 %. At 4 months later, she showed elevated serum creatinine kinase and thus fulfilled the classification criteria of MCTD according to the Ministry of Health, Labor, and Welfare of Japan [4]. At 9 months later, at the age of 11 years, she visited our hospital because of fever, vomitting, and general fatigue lasting for 2 days. She was alert but heavily sweated with cold extremities. Biophysical monitoring showed blood pressure 126/86 mmHg, body temperature 37.1 °C, and SpO_2 98 % on room air. The chest X-ray showed cardiomegaly (CTR 68 %) but no apparent infiltrative shadows. Echocardiography demonstrated right ventricular dilatation, paradoxical movement of the interventricular septum, and tricuspid regurgitation. These findings suggested PAH rather than other causes of pulmonary hypertension such as interstitial lung diseases. Because of failure to access the peripheral vein, we tried to insert a central venous catheter via the femoral vein. During the procedure, electrocardiography showed wide-QRS bradycardia and subsequently asystole. She needed percutaneous cardiopulmonary support for 7 days followed by extracorporeal membrane oxygenation for 4 days. On the sixth hospital day, systolic pulmonary arterial pressure assessed by right heart catheterization was 60 mmHg. Plasma BNP level was 1,146.3 pg/ mL. PAH responded to the combination therapy with epoprostenol sodium, bosentan hydrate, and sildenafil citrate (Fig. 1). Disseminated intravascular coagulation syndrome, pulmonary hemorrhage, and acute renal failure developed but gradually recovered over time. During the course, she lost the distal phalanx of the left forefinger due to ischemic necrosis and suffered from paraplegia, possibly due to infarct of the anterior spinal artery. Although mild ground-glass opacity suggesting IP or lung edema was observed on chest CT scan 1 month after her admission, it subsided following a combination therapy with methylprednisolone pulse therapy (30 mg/kg/dose for three consecutive days) followed by high-dose prednisolone (PSL) (2 mg/kg/day) and three courses of monthly intravenous cyclophosphamide therapy (500 mg/m^2). She was finally discharged from the hospital after 10 months of hospitalization on daily PSL 10 mg/day, azathiopurin 50 mg/day, phosphodiesterase V (PDE-5) inhibitor (tadalafil 20 mg/day), endothelin receptor antagonist (bosentan 62.5 mg/day), and prostacyclin analog (beraprost 300 μg/day). A follow-up echocardiography approximated a systolic pulmonary arterial pressure of 30–35 mmHg. BNP levels decreased and remained within normal range despite residual mild cardiomegaly (CTR 60 %).

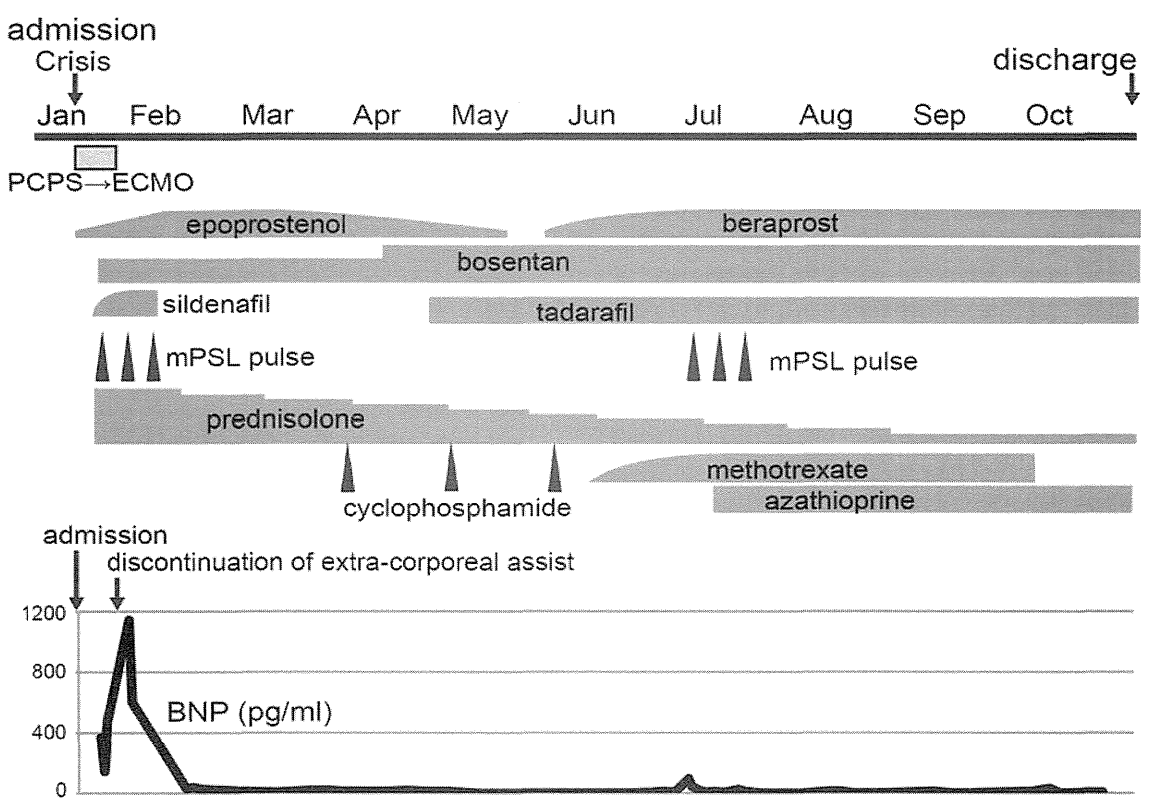

Fig. 1 Treatment and chronological changes in BNP levels. Extracorporeal assist was performed for 11 days since her admission to our hospital. BNP level was first measured on the fifth hospital day during extracorporeal assist. Soon after discontinuation of extracorporeal assist, BNP level was 1,146.3 pg/ mL. *PCPS* percutaneous cardiopulmonary support, *ECMO* extracorporeal membrane oxygenation

Discussion

Although PAH is a life-threatening complication of MCTD, it is difficult to be noted at the asymptomatic phase because early PAH symptoms mimic those of the underlying MCTD [10]. Echocardiography is very helpful for screening for PAH. Heart catheterization is a gold standard for the diagnosis of PAH but is invasive and should be considered when PAH is suspected. PFT is a noninvasive diagnostic test to detect obstructive or restrictive diseases. Particularly, low and decreasing DLCO and %VC/%DLCO ratio≥1.4 are a valuable predictor of the PAH and useful for differential diagnosis from interstitial lung diseases in connective tissue disease (CTD) [9, 11]. Our case showed a low %VC/%DLCO ratio (1.25) and normal echocardiographic and chest CT scan findings at initial examination. Likewise, BNP which is primarily produced by cardiomyocytes of the ventricles of the heart, a biochemical marker for impaired overall cardiac function, was initially near normal levels. These suggest that PAH progressed very rapidly within 1 year after the initial examination. Annual screening of PAH by echocardiography, PFT, and BNP has been recommended in CTD [11]. However, given that PAH may rapidly progress as in our case, routine evaluation should be performed more frequently, e.g., every six months in pediatric MCTD.

Inflammation-mediated organizing vasculopathy are thought to be involved in the progression of CTD-associated PAH. Immunological and/or inflammatory endothelial damage initially leads to vascular obliteration characterized by intimal proliferation, medial hyperplasia, and finally irreversible fibrosis of the small pulmonary arteriole walls [2, 6]. This is supported by the fact that the survival rate of PAH has been improved by an early diagnosis and the prompt use of immunosuppressants in combination with modern PAH-specific vasodilative drugs such as prostanoid, PDE-5 inhibitors, and endothelin receptor antagonist [7, 8]. Consistent with this, the response of PAH to the treatment with both immunosuppressants and vasodilative drugs suggests that the PAH in our case was, at least partially, still reversible. In addition to the slowly progressive inflammatory mechanisms, functional vasospasm due to sympathetic overactivity could be a cause of acute exacerbation of PAH. Invasive procedures could have triggered excessive vasospasms on the basis of underlying subclinically progressed PAH in our case.

Conclusion

Rapidly progressive PAH complicating MCTD was successfully treated with extracorporeal circulation and both vasodilative and immunosuppressive medication. PAH could develop early in the course of pediatric MCTD and needs attention to unexpected acute exacerbation, especially under emotional stress.

Acknowledgments The authors thank all the staffs of Hokkaido University Hospital who participated in the care of the patient.

Conflict of interest The authors have declared no conflicts of interest.

References

1. Burdt MA, Hoffman RW, Deutscher SL, Wang GS, Johnson JC, Sharp GC (1999) Long-term outcome in mixed connective tissue disease: longitudinal clinical and serologic findings. Arthritis Rheum 42:899–909
2. Chatterjee S (2011) Pulmonary hypertension in systemic sclerosis. Semin Arthritis Rheum 41:19–37
3. Kastner B, Kornstadt U, Bach M, Luhrmann R (1992) Structure of the small nuclear RNP particle U1: identification of the two structural protuberances with RNP-antigens A and 70K. J Cell Biol 116:839–849
4. Kasukawa R, Tojo T, Miyawaki S, Yoshida H, Tanimoto K, Nobunaga M, Suzuki T, Takasaki Y, Tamura T (1987) Preliminary diagnostic criteria for classification of mixed connective tissue disease. In: Kasukawa R, Sharp GC (eds) Mixed connective tissue disease and antinuclear antibodies. Elsevier, Amsterdam, pp 41–47
5. Mier RJ, Shishov M, Higgins GC, Rennebohm RM, Wortmann DW, Jerath R, Alhumoud E (2005) Pediatric-onset mixed connective tissue disease. Rheum Dis Clin North Am 31:483–496
6. Nicolls MR, Taraseviciene-Stewart L, Rai PR, Badesch DB, Voelkel NF (2005) Autoimmunity and pulmonary hypertension: a perspective. Eur Respir J 26:1110–1118
7. Sanchez O, Sitbon O, Jais X, Simonneau G, Humbert M (2006) Immunosuppressive therapy in connective tissue diseases-associated pulmonary arterial hypertension. Chest 130:182–189
8. Shirai Y, Yasuoka H, Okano Y, Takeuchi T, Satoh T, Kuwana M (2012) Clinical characteristics and survival of Japanese patients with connective tissue disease and pulmonary arterial hypertension: a single-centre cohort. Rheumatology 51:1846–1854
9. Steen V, Medsger TA Jr (2003) Predictors of isolated pulmonary hypertension in patients with systemic sclerosis and limited cutaneous involvement. Arthritis Rheum 48:516–522
10. Wigley FM, Lima JA, Mayes M, McLain D, Chapin JL, Ward-Able C (2005) The prevalence of undiagnosed pulmonary arterial hypertension in subjects with connective tissue disease at the secondary health care level of community-based rheumatologists (the UNCOVER study). Arthritis Rheum 52:2125–2132
11. Yoshida S (2011) Pulmonary arterial hypertension in connective tissue diseases. Allergol Int 60:405–409

Original Paper

nephron Experimental Nephrology

Nephron Exp Nephrol 2013;124:11–18
DOI: 10.1159/000357356

Received: August 9, 2013
Accepted: November 15, 2013
Published online: January 8, 2014

Prevalence of CD44-Positive Glomerular Parietal Epithelial Cells Reflects Podocyte Injury in Adriamycin Nephropathy

Takayuki Okamoto[a] Satoshi Sasaki[a, b] Takeshi Yamazaki[a] Yasuyuki Sato[a]
Hironobu Ito[a] Tadashi Ariga[a]

[a]Department of Pediatrics, Hokkaido University Graduate School of Medicine, and [b]Department of Pediatrics, Aiiku Hospital, Sapporo, Japan

Key Words
Glomerulosclerosis · Glomerular epithelial cell · Podocytes · CD44 · Osteopontin

Abstract
Background/Aims: Recent study suggests that activation of parietal epithelial cells (PECs) contributes to pathogenesis of glomerulosclerosis and the activation marker CD44 increases in evolving glomerulosclerosis. Here we examined the pathogenic roles of CD44+ epithelial cells in mouse adriamycin nephropathy (ADRN), a representative rodent model for idiopathic focal segmental glomerulosclerosis (FSGS). We also evaluated whether the prevalence of CD44+ PECs reflects different levels of podocyte injuries. ***Methods:*** As a model of FSGS with different degrees of podocyte injury, ADRN models in mice of different ages were utilized. Immunohistochemistry and immunofluorescence were used to determine roles of CD44 expression. ***Results:*** By immunohistochemistry, CD44 expression became positive in claudin-1+ PECs and an increase in CD44+ PECs was associated with reduced expression of synaptopodin and podocin in diseased glomeruli. Furthermore, immunofluorescence staining demonstrated co-expression with osteopontin, a CD44 ligand that plays a significant role in the progression of glomerulosclerosis, thereby suggesting interactions between these molecules. Analysis of the number of WT-1+ podocytes and the levels of electron microscopic foot process effacement revealed a milder degree of podocyte injury in younger ADRN models compared to older ones. Comparative immunohistochemical analysis indicated that the prevalence of CD44+ PECs consistently reflects different degrees of podocyte injury within each different-aged ADRN model. ***Conclusion:*** CD44+ PECs play significant roles in progressive glomerulosclerosis and the prevalence of the cells reflects different degrees of podocyte injury in ADRN.

Introduction

Focal segmental glomerulosclerosis (FSGS) is a major cause of end-stage kidney disease. Key in the pathogenesis of FSGS is loss or dysfunction of podocytes [1–4] originating from various congenital or acquired etiologies [5, 6]. Following podocyte injuries, sequential pathological events such as podocyte loss resulting in denudation of glomerular basement membrane, formation of Bowman's capsule (BC) adhesion intervened with invaded parietal epithelial cells (PECs), and finally scar formation occur to form FSGS [2, 7].

CD44, a class I transmembrane glycoprotein, has previously been implicated in cell-cell adhesion and cyto-

KARGER

1660–2129/14/1244–0011$39.50/0

E-Mail karger@karger.com
www.karger.com/nee

Takayuki Okamoto, MD, PhD
Department of Pediatrics
Hokkaido University Graduate School of Medicine
N15, W7, Sapporo 060-8638 (Japan)
E-Mail okamon@med.hokudai.ac.jp

Table 1. Metabolic, physiologic, and histopathologic parameters in ADRN mice in different ages

	Control (12-week-old)		12-week-old ADRN		Control (6-week-old)		6-week-old ADRN	
	day 14	day 28	day 14	day 28	day 14	day 28	day 14	day 28
Body weight, g	26.5±1.6	27.3±2.0	22.2±1.8**	20.8±1.5**	26.0±0.1	24.5±1.6	20.0±1.6*	17.6±1.2**
S-creatinine, mg/dl	0.08±0.01	0.07±0.02	0.09±0.01	0.10±0.02*	0.11±0.01	0.08±0.01	0.09±0.01	0.10±0.01
Urinary protein to creatinine ratio, g/g·Cr	18.2±1.0	13.7±8.3	30.2±12.1	33.8±14.7*	11.8±1.0	20.7±4.2	27.0±3.7*	18.3±11.9
Glomerulosclerosis, % glomeruli	1.5±1.1	0.7±0.6	2.3±1.8	6.6±3.1*	0.2±0.1	0.3±0.2	1.9±1.7	2.9±4.1*,##
Crescent, % glomeruli	0.0±0.0	0.0±0.0	1.6±1.3	9.8±2.6*	0.0±0.0	0.0±0.0	1.3±1.5	3.1±2.8*,#

Data given a mean ± SD. n = 6, representing numbers of mice used. * $p < 0.05$, ** $p < 0.01$ versus age-matched controls, # $p < 0.05$, ## $p < 0.01$ versus 12-week-old ADRN mice.

skeletal rearrangements, as well as cell signaling, cell survival, and malignant transformation [8]. A few studies first focused on upregulation of CD44 expression in inflammatory renal diseases with tubulointerstitial injuries [9]. Recently, several investigations have indicated the potential role of CD44 in the progression of glomerular injury, especially in the activation of PECs [10, 11].

In this study, we attempted to further clarify the role of CD44 expressed by resident glomerular cells in the process of glomerulosclerosis. As a model for FSGS characterized by progressive podocyte injuries [12], we utilized an adriamycin nephropathy (ADRN) model in mice of different ages. The glomerular localization of CD44 and its ligand, osteopontin (OPN), was studied during the course of glomerulosclerosis and the relationship between the degrees of podocyte injury and glomerular CD44 expression was examined.

Materials and Methods

Animals

Male BALB/c mice were purchased from Sankyo Lab Service (Tokyo, Japan) and received tail vein injection of adriamycin (ADR; doxorubicin hydrochloride; Kyowa Hakko, Tokyo, Japan) at a dose of 12 mg/kg. To evaluate CD44 expression with different degrees of severity of the glomerular injuries, we utilized age-related differences in susceptibility to ADR as reported elsewhere [12, 13]. The experimental groups are: the mice received ADR injection when 12 weeks old (referred to as the 12-week-old ADRN model), the mice received ADR injection when 6 weeks old (the 6-week-old ADRN model), and age-matched controls injected with equal volumes of isotonic saline. Serum, urine and kidneys were sequentially collected at sacrifice on days 0, 5, 7, 10, 14, and 28, considering day 0 when ADR was injected (n = 6 per group at each time point). In the 12-week-old ADRN mice, body weight loss, significant levels of proteinuria and progressive renal dysfunction had been observed by day 28 compared with the control group (table 1). Histopathologic analysis demonstrated a significant increase over controls in the percentage of glomeruli involved by segmental or global sclerosis and crescents. In contrast to the 12-week-old model, 6-week-old model mice showed milder degrees of body weight loss, renal dysfunction and proteinuria. Concurring with the clinical data, the 6-week-old model also showed less histopathologic injuries. All care of mice was conducted in accordance with Guidelines for the Care and Use of Laboratory Animals at the Hokkaido University.

Kidney Functional Parameters

Urine and blood samples were obtained at the time of sacrifice. Urinary levels of protein, creatinine and serum levels of total protein and creatinine were determined at SRL, Inc. (Tokyo, Japan).

Morphological Analysis and Evaluation of Glomerular Injuries

Paraffin-embedded kidney sections 3 μm in thickness were stained with hematoxylin and eosin or periodic acid-Schiff for morphological analysis. The percentage of glomeruli containing lesions such as sclerosis, adhesions or hyperplasia of the glomerular epithelial cells, were assessed by counting the total number of glomeruli in a representative section from at least 50 glomeruli per mouse. We defined glomerular epithelial cells of two or more layers in the urinary space as crescents.

For electron microscopy (EM), kidneys were fixed with 2.5% glutaraldehyde in PBS, postfixed in 1% osmium tetroxide in PBS, dehydrated in a graded series of ethanol dilutions, and embedded in Epoxy Resin 812 (Oken, Tokyo, Japan). Ultrathin sections for EM were stained with uranyl acetate and lead citrate and were examined with a JEM 1220 (JEOL, Tokyo, Japan). Podocyte foot process effacement (FPE) was evaluated in at least 5 glomeruli per mouse. The degree of effacement was quantified using ratios of cumulative FPE width to a length of glomerular basement membrane. Images were analyzed with the NIH Image J software.

Immunohistochemistry and Immunofluorescence Studies

The primary antibodies used were as follows: rat anti-mouse CD44 antibody (1:500; Bio Legend, San Diego, Calif., USA), goat anti-mouse OPN antibody (1:50; Santa Cruz Biotech, Santa Cruz,

Calif., USA), rabbit anti-mouse Wilms' tumor (WT)-1 antibody (1:50; Santa Cruz Biotech), goat anti-mouse synaptopodin antibody (1:200; Sigma Chemical Co., St. Louis, Mo., USA) and rabbit anti-mouse podocin antibody (1:50; Sigma), rabbit anti-mouse claudin-1 antibody (1:50; Abcam, Inc., Cambridge, Mass., USA).

For immunofluorescence (IF), frozen sections 4 μm in thickness were used. The sections were incubated with primary antibodies for 16 h at 4°C, and subsequently exposed to corresponding FITC-, Cy3- or Cy5-conjugated secondary antibodies. The secondary antibodies used were FITC-conjugated goat anti-rat IgG (BD Biosciences, San Jose, Calif., USA), Cy3-conjugated donkey anti-rabbit IgG, anti-goat IgG, and Cy5-conjugated donkey anti-goat IgG (Jackson Immunoresearch Laboratories, West Grove, Pa., USA). The stained sections were examined in an epifluorescent microscope (Olympus BX60). For double or triple IF labeling, the slides were examined with confocal laser microscopes (Biorad MRC1024 and Olympus fluoview FV10i) after serial incubation with appropriate primary and secondary antibodies.

For immunohistochemistry (IHC), kidneys were immersion-fixed in 4% paraformaldehyde-lysin-periodate. After blocking with 0.3% H_2O_2 in methanol at room temperature, the sections were incubated with the appropriate dilution of primary antibodies at 4°C overnight. The sections were subsequently incubated with Histofine simple-stain mouse MAX-PO RAT (Nichirei, Tokyo, Japan), peroxidase-conjugated swine anti-rabbit IgG, or rabbit anti-goat IgG (Dako, Glostrup, Denmark) to detect antigens (CD44, OPN, synaptopodin, and WT-1). Color detection was performed using DAB as a chromogen. Negative controls were obtained by omission of primary antibodies. The number of podocytes per glomerulus was calculated as the WT-1-positive nuclei per glomerulus. The glomerular tuft area measured with a digital imaging analysis (Olympus DP2-BSW, Japan) was used as the denominator for the number of positively stained podocytes [14]. The staining of glomerular CD44 expression was defined by the percentage of glomeruli with expression to all. All measurements were assessed by counting the total number of glomeruli in a representative section from at least 50 glomeruli per mouse.

Statistical Analysis

Each bar represents the mean ± SD in each group. The difference between control and treated groups was assessed by the unpaired Student's t test, except for semiquantitative data, which were analyzed by the Mann-Whitney U test. Values of $p < 0.05$ were considered significant. For comparison of more than three groups, analysis of variance (ANOVA) was used. If the ANOVA was significant, the Student-Newman-Keuls test was used as a post hoc test.

Results

Glomerular CD44 Expression in 12-Week-Old ADRN Mice

CD44 expression was first examined in kidneys of the 12-week-old ADRN by IHC (fig. 1). Although immunoperoxidase staining demonstrated a few CD44-positive cells in the interstitium, CD44 expression was rarely observed in the glomeruli of control mice until day 28. In

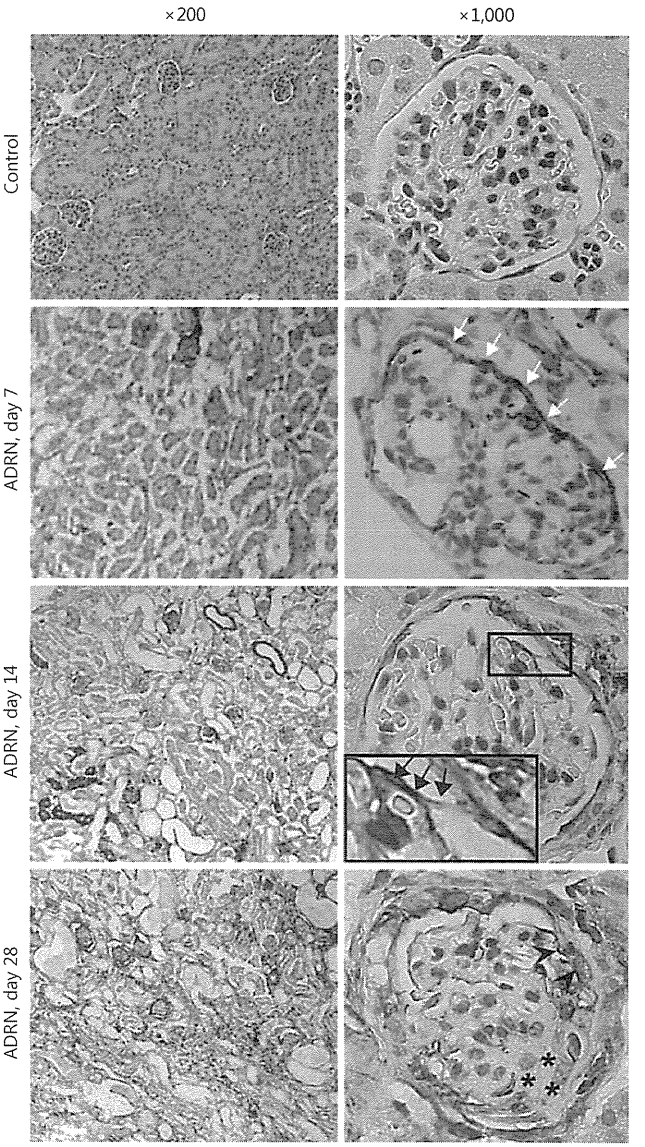

Fig. 1. Immunohistochemical detection of CD44 expression in ADRN. Representative IHC staining of kidney sections from 12-week-old ADRN and control mice is shown at low (left panels) and high magnification (right panels). CD44 expression is almost negative in control mice until day 28 after saline injection. In ADRN mice, the cells lining BC of a few corticomedullary glomeruli show positive for CD44 from day 7 (white arrows). At day 14, CD44 expression is increased and bridging epithelial cells positive for CD44 were occasionally observed (black arrows). At day 28, CD44 expression is prominent and positive staining is observed at the site of BC adhesion (arrowheads) in a glomerulus with segmental sclerosis (asterisks).

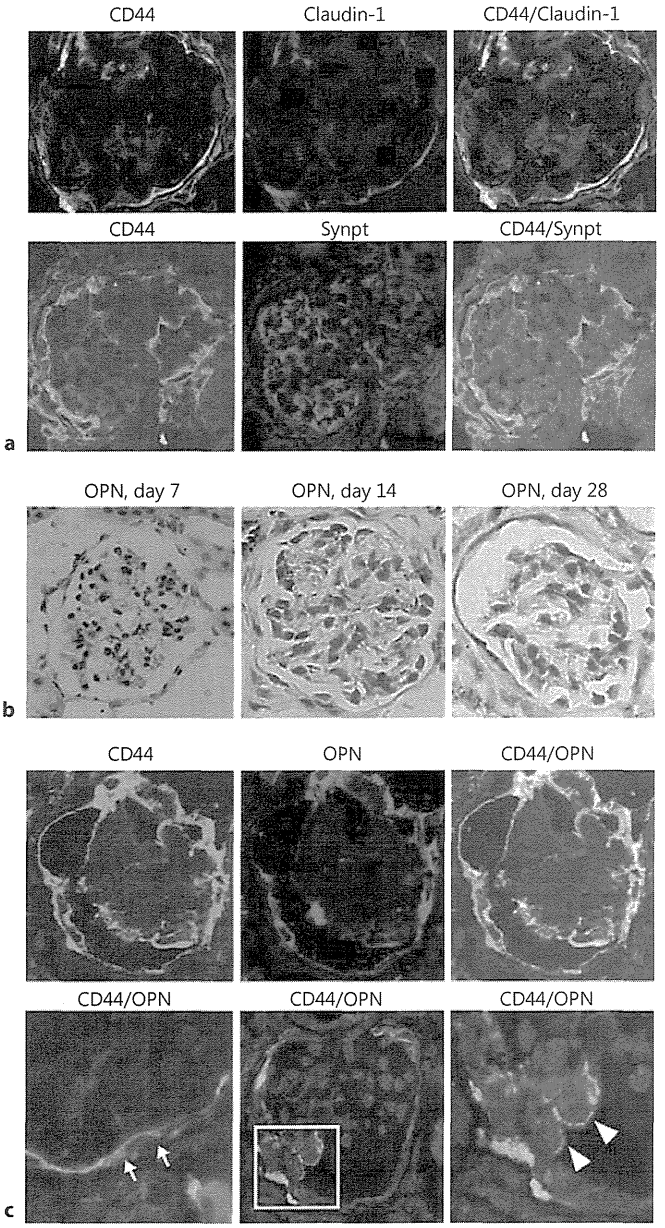

Fig. 2. Characterization of the glomerular resident cells expressing CD44. **a** Confocal double IF labeling CD44-claudin-1 or CD44-synaptopodin (Synpt) on glomerular sections from ADRN. **b** OPN expression in ADR-injured glomeruli. In representative IHC analysis of kidney sections from 12-week-old ADRN mice at day 7, 14, or 28. OPN expression is detected in some PECs from day 14. **c** Confocal double IF labeling CD44-OPN on kidney sections from 12-week-old ADRN at day 28. Co-expression of CD44 and OPN is shown. Co-localization of these proteins is also observed in the cells covering the capillary tuft together with the co-expression of the proteins in PECs on the opposite side (upper panels). The cells showing perinuclear cytoplasmic expression of OPN with perimembranous expression of CD44 (arrows) and the bridging-like cells positive for these proteins (arrowheads) are shown.

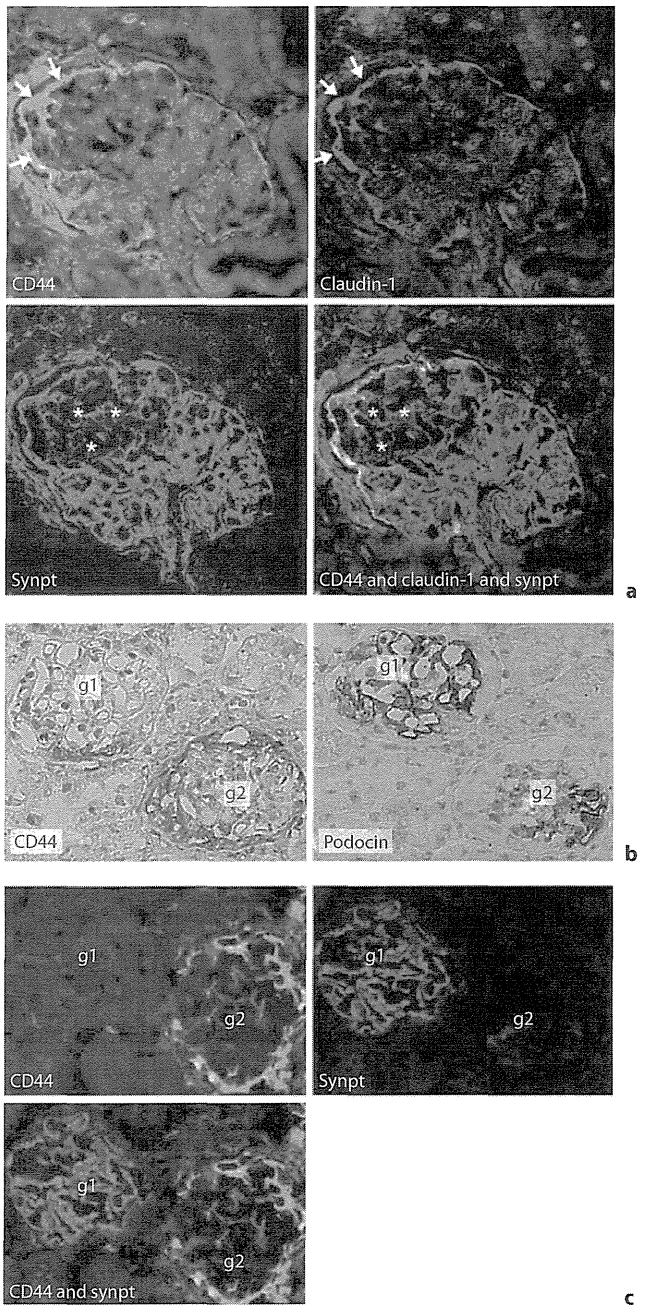

Fig. 3. Confocal IF and IHC analysis of relationship between de novo CD44 expression by PECs and expression of podocyte markers in ADR-injured glomeruli. **a** Triple IF staining for CD44 (green; FITC), claudin-1 (red; Cy3) and synaptopodin (Synpt) (blue; Cy5). Note the claudin-1+ CD44+ PECs along the capillary tufts (arrows) with reduced expression of synaptopodin (asterisks). **b** IHC staining for CD44 (left panel) and podocin (right panel) in serial sections. Note the reciprocal expression patterns of these proteins in adjacent glomeruli (g1, g2). **c** Double IF staining for CD44 and synaptopodin. Differential expression pattern of the podocyte markers (podocin and synaptopodin) and CD44 in adjacent glomeruli (g1, g2) of the ADRN mice is shown.

the ADRN mice, CD44 expression was becoming positive in the cells lining BC of a few corticomedullary glomeruli from day 7 (fig. 1, white arrows). Thereafter the number of CD44-positive cells increased in glomeruli, tubules and interstitium together with an upregulation of the staining intensity. In addition, bridging epithelial cells between BC and the capillary tuft occasionally demonstrated positive for CD44 (fig. 1, black arrows). Quantification of IHC preparations showed a significant increase in the number of CD44-positive glomeruli in the ADRN mice over controls from day 10 (see fig. 4d).

Characterization of CD44-Positive Glomerular Cells by Confocal Analysis

To further characterize the CD44-positive glomerular cells in FSGS, confocal IF was performed using several specific markers of PECs and podocytes (fig. 2a). CD44-positive cells showed co-expression with the PEC marker claudin-1, but co-expression with the specific markers of podocytes, synaptopodin, was not seen. These results suggest that CD44-positive cells in ADR-diseased glomeruli are mainly composed of claudin-1+ PECs, whereas synaptopodin+ podocytes do not express CD44.

Glomerular Co-Localization of CD44 and OPN Expression in ADRN Mice

We examined the expression of OPN, known to be a protein ligand of CD44, by IHC. In 12-week-old ADRN, OPN expression was observed from day 14 in cells infiltrating the interstitium, tubules and some PECs (fig. 2b). Confocal analysis demonstrated perinuclear cytoplasmic expression of OPN with perimembranous expression of CD44 in some PECs within the injured glomeruli (fig. 2c, arrows). In some glomeruli, co-localization of CD44 and OPN was also observed in the cells covering the capillary tuft together with the co-expression of the proteins in PECs on the opposite side (fig. 2). Bridging-like cells positive for these proteins were occasionally detected between BC and capillary tufts (fig. 2, arrowheads).

Relationship between the Degrees of Podocyte Injuries and Glomerular CD44 Expression

By triple IF staining for CD44, claudin-1 and synaptopodin, claudin-1+ CD44+ PECs were occasionally observed along the capillary tufts (fig. 3a, arrows) with reduced expression of synaptopodin (fig. 3a, asterisks). Differential expression pattern of the podocyte markers (podocin and synaptopodin) and CD44 was clearly shown in adjacent glomeruli of the ADRN mice by IHC (fig. 3b, c). While CD44 was expressed in the glomerular lesions with a reduced expression of podocyte markers, the glomeruli with normal expression of podocyte markers were negative for CD44.

To clarify the relationship between the degrees of podocyte injuries and glomerular CD44 expression in FSGS, we evaluated two different models, the conventional 12-week-old ADRN and the 6-week-old ADRN. As shown in table 1, the 6-week-old ADRN represent a milder degree of ADR-induced podocyte injuries compared with 12-week-old ADRN. Podocyte number was evaluated by quantification of the number of WT-1+ cells in the glomerular tuft, using calculated glomerular tuft area (mm^2) as the denominator [14]. From day 10, the numbers of podocyte/mm^2 in tuft were significantly decreased in 12-week-old ADRN (fig. 4b). EM study demonstrated a significant increase in the percentage of FPE from day 7 (fig. 4c). In contrast, the number of CD44-positive glomeruli was significantly increased from day 10 (fig. 4d). In 6-week-old ADRN, podocyte number/mm^2 in tuft showed decreasing temporal trends at day 7; however, the number was relatively steady until day 28 and showed no difference compared to controls (fig. 5a). On the other hand, the changes in glomerular CD44 expression in the 6-week-old model demonstrated an interesting pattern such as a rapid increase of glomerular CD44 expression from day 7 (fig. 5b). Moreover, the phase of increased CD44 expression in 6-week-old model mice occurred much earlier than in the 12-week-old model (fig. 5b). Although the peaked expression of CD44 was at day 28 in 6-week-old model mice as well as in the 12-week-old model, the peak was much higher in the older mice.

Discussion

Our findings show that prevalence of CD44+ PECs reflects progression of podocyte injury in the course of ADRN, a representative rodent model for FSGS. The results demonstrated that glomerular CD44 expression appears from the early phase of podocyte injury and the CD44+ glomerular cells are mainly composed of PECs. Furthermore, bridging-like cells between BC and capillary tufts were positive for CD44 expression, and the CD44+ PECs occasionally invade into capillary tufts with significant loss of podocyte markers. Using age-different models, we demonstrated that prevalence of CD44+ PECs consistently reflects degrees of podocyte injury.

CD44 is a family of multifunctional glycoproteins involved in cell-cell and cell-matrix interactions, cell traf-

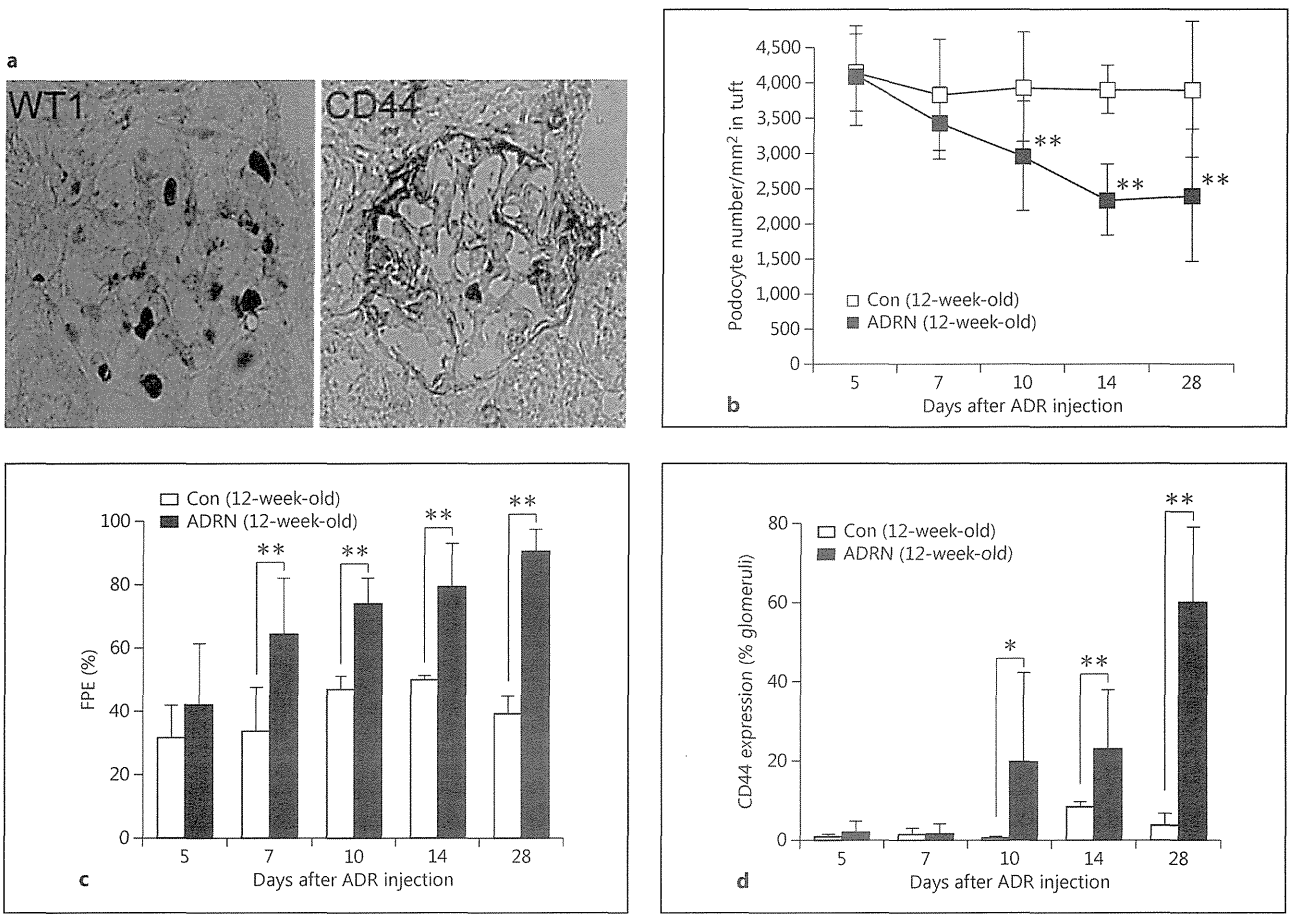

Fig. 4. Time course analysis of glomerular CD44 expression and podocyte injury in 12-week-old ADRN. **a** Representative IHC for WT-1 and CD44 in serial sections of ADR-injured glomeruli. **b** Quantitation of WT-1+ cells/mm^2 glomerular tuft area during time course of 12-week-old ADRN. Note the decrease of WT-1+ cells/mm^2 glomerular tuft from day 10 compared with control mice ($p < 0.01$). **c** Degree of podocyte FPE during time course of ADRN. A significant increase over controls in the percentage of FPE is observed from day 7 ($p < 0.01$). **d** Glomerular CD44 expression during time course of ADRN from day 5 to day 28 after ADR injection. Note the increase of the number of CD44+ glomerular cells from day 10 ($p < 0.05$). * $p < 0.05$, ** $p < 0.01$.

ficking, lymph node homing and the presentation of growth factors/cytokines/chemokines to coordinate signaling events [15]. Using experimental models of crescentic glomerulonephritis and collapsing glomerulopathy, Smeets et al. [11] first found that CD44+-activated PECs plays a major role in the formation of extracapillary cellular lesions. Recently they also demonstrated that CD44+-activated PECs contribute to the formation of sclerotic lesions using the transgenic mouse models for FSGS and the MWF rats [16].

To further investigate pathologic roles of activated PECs in FSGS, we used ADRN mice characterized by a gradual progression of podocyte apoptosis leading to formation of FSGS. Our results demonstrated that CD44 expression appears from the early phase (day 7 after ADR injection) of ADR-induced glomerular injury and the CD44+ glomerular cells are mainly composed of PECs. As a previous report describes that the number of apoptotic podocytes peaks from day 3 after ADR injection [17], CD44+-activated PECs may respond to successive podocyte depletion from early phase after ADR injection. In addition, we observed bridging epithelial cells between BC and the capillary tuft occasionally demonstrated positive for CD44. By triple IF staining, CD44+ PECs was observed along capillary tufts where expression of the podocyte marker, synaptopodin, was reduced. These re-

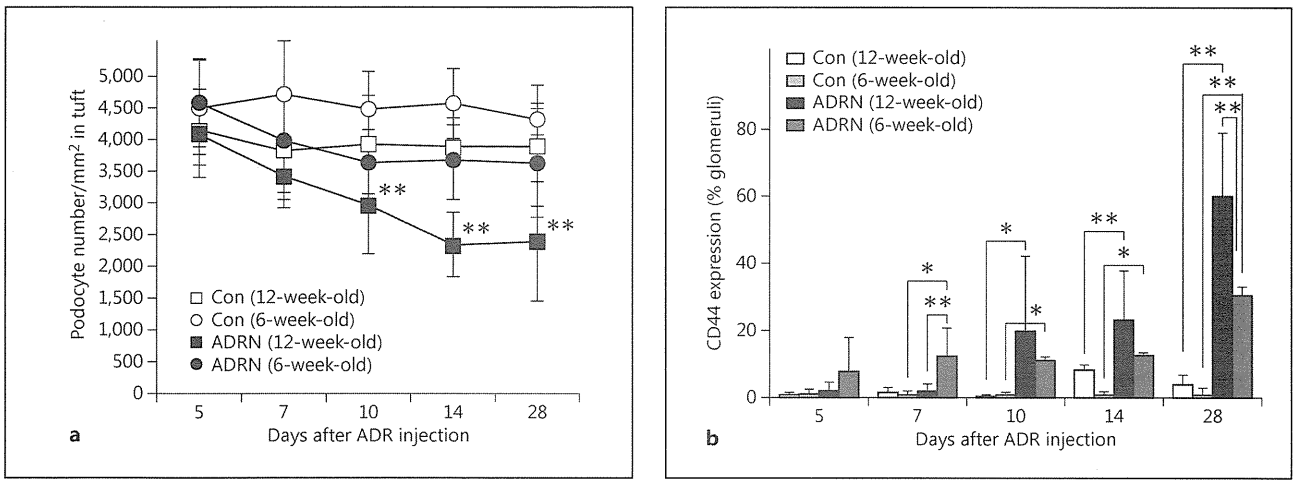

Fig. 5. Comparative analysis of time course of glomerular CD44 expression and WT-1+ podocyte numbers in different-aged ADRN mice model. **a** Time course analysis of WT-1+ cells/mm^2 glomerular tuft area in 12- and 6-week-old ADRN and the age-matched controls. **b** Time course analysis of glomerular CD44 expression in 12- and 6-week-old ADRN and the age-matched controls. The decrease of WT1+ cells/mm^2 in tuft is not significant in 6-week-old ADRN until day 28, whereas the significant decrease is observed in 12-week-old ADRN. The changes in glomerular CD44 expression in the 6-week-old ADRN show a rapid increase of glomerular CD44 expression from day 7; however, the peaked expression of CD44 in 6-week-old ADRN is much lower from day 14. Values are expressed as mean ± SD. * $p < 0.05$, ** $p < 0.01$.

sults support a possibility that PECs migrate from BC to the capillary tuft for replacement of lost podocytes in glomerular disorders [16, 18]. Furthermore, a pattern of differential expression of CD44 and podocyte markers was clearly shown in adjacent glomeruli suggesting that CD44+-activated PECs reflect podocyte injury during the formation of sclerotic lesions in FSGS.

OPN, a cell adhesion and migration molecule, has been known to play significant roles in the progression of glomerulosclerosis [19–21]. In this study, we observed increased OPN expression in CD44+ PECs in ADR-diseased glomeruli. The result suggests that CD44-mediated cell motility may have a significant role in PEC migration through the interactions with OPN, and functionally related molecules [22, 23]. Thus, further studies are needed to determine the functional significance of OPN/CD44 interaction in PEC activation.

In the present study, we also found that the level of glomerular CD44 expression well reflects podocyte depletion during the time course of FSGS in the 12-week-old model. To obtain a clearer definition of the association between CD44+ PECs and podocyte injury, we further assessed ADRN models with different degrees of podocyte injury. To that end, we utilized the ADRN mice of different ages, 12- and 6-week-old, because the differences in age as well as sex and strains of mice in susceptibility to ADR had already been recognized [12]. In this comparative analysis, the 6-week-old model mice demonstrated less severe glomerular injury and the expression levels of podocyte markers were relatively steady, suggesting milder degrees of ADR-induced podocyte injury compared with the 12-week-old model. Consistent with a milder degree of podocyte injury, the peaked CD44 expression in PECs was relatively lower in the 6-week-old model. Furthermore, the 6-week-old ADRN showed earlier changes in podocyte depletion reflected by a rapid increase of CD44+ PECs. Therefore, our study indicates that the prevalence of CD44 expression in PECs reflects different degrees of podocyte injury during the course of FSGS. Our results also support recent findings in transplant patients [24], suggesting CD44 positivity in PECs is a good marker for recurrent FSGS. Although the ADRN is a well-established experimental model for successive progression of histologic injuries in FSGS, the model has a limitation for a separate analysis of injuries in both types of glomerular epithelial cells. Further accumulative studies will be necessary to disclose the cross-talk between PECs and podocytes.

In summary, our study suggests that the prevalence of CD44+ PECs reflects different degrees of podocyte injury

in the progression of glomerulosclerosis. CD44-mediated cell motility may have a significant role in PEC migration through the interactions with functionally related molecules such as OPN. More studies are needed to further examine the pathologic roles of CD44 expression in activated PECs.

Acknowledgements

This work was supported by grants to S.S. from the Japan Society for the Promotion of Science (19590928 and 23591176). This work was also supported in part by the Chugai Science Foundation. Part of this work was presented at the 43rd Annual Scientific Meeting of the American Society of Nephrology, November 20, 2010, Denver, Colo., USA.

Disclosure Statement

The authors have no conflicts of interest to disclose.

References

1 Mundel P, Shankland SJ: Podocyte biology and response to injury. J Am Soc Nephrol 2002;13:3005–3015.

2 Kriz W, Gretz N, Lemley KV: Progression of glomerular diseases: Is the podocyte the culprit? Kidney Int 1998;54:687–697.

3 Wharram BL, Goyal M, Wiggins J, Kershaw D, Wiggins R: Podocyte depletion causes glomerulosclerosis: diphtheria toxin-induced podocyte depletion in rats expressing human diphtheria toxin receptor transgene. J Am Soc Nephrol 2005;16:2941–2952.

4 Tryggvason K, Patrakka J, Wartiovaara J: Hereditary proteinuria syndrome and mechanisms of proteinuria. N Engl J Med 2006;354:1387–1401.

5 Kim YH, Goyal M, Kurnit D, Wharram B, Wiggins J, Holzman L, Kershaw D, Wiggins R: Podocyte depletion and glomerulosclerosis have a direct relationship in the PAN-treated rat. Kidney Int 2001;60:957–968.

6 Wiggins RC: The spectrum of podocytopathies: a unifying view of glomerular diseases. Kidney Int 2007;71:1205–1214.

7 Smeets B, Dijkman HB, Wetzels JF, Steenbergen EJ: Lessons from studies on focal segmental glomerulosclerosis: an important role for parietal epithelial cells? J Pathol 2006;210:263–272.

8 Ponta H, Sherman L, Herrlich PA: CD44: from adhesion molecules to signaling regulators. Nat Rev Mol Cell Biol 2003;4:33–45.

9 Benz PS, Fan X, Wuthrich RP: Enhanced tubular epithelial CD44 expression in MRL-lpr lupus nephritis. Kidney Int 1996;50:156–163.

10 Florquin S, Nunziata R, Claessen N, van den Berq FM, Pals ST, Weening JJ: CD44 expression in IgA nephropathy. Am J Kidney Dis 2002;39:407–414.

11 Smeeets B, Uhlig S, Fuss A, Mooren F, Wetzels JF, Floege J, Moeller MJ: Tracing the origin of glomerular extracapillary lesions from parietal epithelial cells. J Am Soc Nephrol 2009;20:2604–2615.

12 Pippin JW, Brinkkoetter PT, Cormack-Aboud FC, Durvasula RV, Hauser PV, Kowalewska J, Krofft RD, Logar CM, Marshall CB, Ohse T, Shankland SJ: Inducible rodent models of acquired podocyte disease. Am J Physiol Renal Physiol 2009;296:F213–F229.

13 Hahn H, Park YS, Ha IS, Cheong HI, Choi Y: Age-related differences in adriamycin-induced nephropathy. Pediatr Nephrol 2004;19:761–766.

14 Zhang J, Hansen KM, Pippin JW, Chang AM, Taniguchi Y, Krofft RD, Pickering SG, Liu ZH, Abrass CK, Shankland SJ: De novo expression of podocyte proteins in parietal epithelial cells in experimental aging nephropathy. Am J Physiol Renal Physiol 2012;302:F571–F580.

15 Sanchez-Nino MD, Sanz AB, Ruiz-Andres O, Poveda J, Izquierdo MC, Selgas R, Eqido J, Ortiz A: MIF, CD74 and other partners in kidney disease: tales of a promiscuous couple. Cytokine Growth Factor Rev 2013;24:23–40.

16 Smeets B, Kuppe C, Sicking EM, Fuss A, Jirak P, van Kuppevelt TH, Endlich K, Wetzels JF, Grone HJ, Floege J, Moeller MJ: Parietal epithelial cells participate in the formation of sclerotic lesions in focal segmental glomerulosclerosis. J Am Soc Nephrol 2011;22:1262–1274.

17 Asanuma K, Akiba-Takagi M, Kodama F, Asao R, Nagai Y, Lydia A, Fukuda H, Tanaka E, Shibata T, Takahara H, Hidaka T, Asanuma E, Kominami E, Ueno T, Tomino Y: Dendrin location in podocytes is associated with disease progression in animal and human glomerulopathy. Am J Nephrol 2011;33:537–549.

18 Lasagni L, Romagnani P: Glomerular epithelial stem cells: the good, the bad, and the ugly. J Am Soc Nephrol 2010;21:1612–1619.

19 Wang KX, Denhardt DT: Osteopontin: role in immune regulation and stress responses. Cytokine Growth Factor Rev 2008;19:333–345.

20 Nicholas SB, Liu J, Kim J, Ren Y, Collins AR, Nquyen L, Hsueh WA: Critical role for osteopontin in diabetic nephropathy. Kidney Int 2010;77:588–600.

21 Kramer AB, Ricardo SD, Kelly DJ, Waanders F, van Goor H, Navis G: Modulation of osteopontin in proteinuria-induced renal interstitial fibrosis. J Pathol 2005;207:483–492.

22 Weber GF, Ashkar S, Glimcher MJ, Cantor H: Receptor-ligand interaction between CD44 and osteopontin (Eta-1). Science 1996;271:509–512.

23 Zohar R, Suzuki N, Arora P, Gloqauer M, McCulloch CA, Sodek J: Intracellular osteopontin is an integral component of the CD44-ERM complex involved in cell migration. J Cell Physiol 2000;184:118–130.

24 Fatima H, Moeller MJ, Smeets B, Yang HC, D'Agati VD, Alpers CE, Fogo AB: Parietal epithelial cell activation marker in early recurrence of FSGS in the transplant. Clin J Am Soc Nephrol 2012;7:1852–1858.

In the United States the regulation of nonstandardized AEs presented some similarities with our approach. AEs were classified into 4 categories according to scientific data supporting their use in diagnosis and treatment, and the extracts were regularly evaluated by the regulatory agencies. The last update was conducted between 2003 and 2011, and the process was recently reviewed by Slater et al.[1] It was shown that for nearly half of nonstandardized AEs there were, in fact, little or no data to support their effectiveness. We had similar results: 66 of 84 AEs were validated for diagnosis, but only for 29 of 66 was there at least 1 published piece of data to support their effectiveness for immunotherapy (Table I). Among those 66 authorized AEs, approximately one third are standardized. There is no consensus about the standardization methods, and the European approaches present some differences compared with the US approach (see Table E1 in this article's Online Repository at www.jacionline.org). Briefly, in-house reference preparation (IHRP) AEs are standardized *in vivo* and *in vitro*. Each manufacturer has its own IHRP, and there is no national standard. Batch-to-batch standardization is performed *in vitro* through a comparison of the AEs with the IHRP.[9]

In the future, the NPP list will be updated every 5 years, and requests for MA will be made and processed for standardized AEs produced industrially and frequently used for immunotherapy.

In conclusion, for the first time in Europe, this work guarantees that available AEs are clinically relevant and safe. Moreover, it guarantees that all AEs comply with recent European guidelines on APs, including rare allergens for which it is not possible to obtain large clinical studies requested for MA. The process involved all the representatives of allergists and manufacturers and is still ongoing.

Frédéric de Blay, MD[a,b]
Virginie Doyen, MD[b,c]
Evelyne Bloch-Morot, MD[d]
Daniel Caillot, MD[e]
Jacques Gayraud, MD[f]
Aymar de Laval, MD[e]
Alain Thillay, MD[g]
*for the APSI group**

From [a]the French Society of Allergology (SFA), Paris, France; [b]the Division of Allergy, Department of Respiratory Disease, University Hospital of Strasbourg and University of Strasbourg, Strasbourg, France; [c]the Clinic of Immuno-Allergology, CHU Brugmann, Université Libre de Bruxelles (ULB), Brussels, Belgium; [d]the French Association for Continual Medical Education of Allergists (ANAFORCAL), Aix-en-Provence, France; [e]the French Committee of Support (Comite de Soutien de l'Allergologie), Clermont-Ferrand, France; [f]the French Trade Union of Allergists (SNAF), Tarbes, France; and [g]the Trade Union of Allergists (ANAICE), Tours, France. E-mail: Frederic.deblay@chru-strasbourg.fr.

*APSI group: I. Bosse, La Rochelle; J. C. Farouz, Bordeaux, ANAICE, France; M. Epstein, C. Martens, Paris, SNAF, France; P. Demoly, Inserm U657, CHU de Montpellier, Montpellier; A. Didier, CHU de Toulouse, Toulouse, French Society of Allergology.

Disclosure of potential conflict of interest: F. de Blay and A. de Laval have received research support from Stallergènes and ALK-Abelló. The rest of the authors declare that they have no relevant conflicts of interest.

REFERENCES

1. Slater JE, Menzies SL, Bridgewater J, Mosquera A, Zinderman CE, Ou AC, et al. The US Food and Drug Administration review of the safety and effectiveness of nonstandardized allergen extracts. J Allergy Clin Immunol 2012;129:1014-9.
2. Slater JE. Standardized allergen vaccines in the United States. Clin Allergy Immunol 2008;21:273-81.
3. Directive 2001/83/EC of the European Parliament and of the Council of 6 November 2001 on the Community code relating to medicinal products for human use. Available at: http://eur-lex.europa.eu/LexUriServ/LexUriServ.do?uri=OJ:L:2001:311:0067:0128:EN:PDF. Accessed July 2, 2009.
4. Lorenz AR, Lüttkopf D, Seitz R, Vieths S. The regulatory system in Europe with special emphasis on allergen products. Int Arch Allergy Immunol 2008;147:263-75.
5. Summary of the response to the questionnaire marketing authorization of allergen products in Europe sent to national regulatory agencies. Arb Paul Ehrlich Inst Bundesamt Sera Impfstoffe Frankf A M 2006;(95):43-4.
6. Kaul S, May S, Lüttkopf D, Vieths S. Regulatory environment for allergen-specific immunotherapy. Allergy 2011;66:753-64.
7. Ministère de la santé et des solidarités. Décret n° 2004-188 du 23 février 2004 relatif aux allergènes préparés spécialement pour un seul individu et modifiant le code de la santé publique. OJ 200;50:4101 texte n° 30.
8. European Medicine Agency (EMEA), Committee for Medicinal Products for Human Use (CHMP) and Biologics Working Party (BWP): guideline on allergen products: production and quality issues, 2007; EMEA/CHMP/BWP/304831/2007. Available at: http://www.pei.de/cln_227/nn_162408/EN/medicinal-products/allergens/allergens-node.html?__nnn=true Accessed May 1, 2012.
9. Larsen JN, Dreborg S. Standardization of allergen extracts. Methods Mol Med 2008;138:133-45.

Available online January 30, 2013.
http://dx.doi.org/10.1016/j.jaci.2012.11.003

Common variable immunodeficiency classification by quantifying T-cell receptor and immunoglobulin κ-deleting recombination excision circles

To the Editor:

Common variable immunodeficiency (CVID) is the most frequent primary immunodeficiency associated with hypogammaglobulinemia and other various clinical manifestations. CVID was originally reported to be a disease primarily caused by defective B-cell function, with defective terminal B-cell differentiation rendering B cells unable to produce immunoglobulin. However, combined immunodeficiency (CID) involving both defective B and T cells is often misdiagnosed as CVID.[1] Indeed, one study reported that $CD4^+$ T-cell numbers were decreased in 29% of 473 patients with CVID[2]; similarly, another study found that naive T-cell numbers were markedly reduced in 44% (11/25) of patients with CVID.[3] These observations indicated that a subgroup of patients with clinically diagnosed CVID is T-cell deficient. Consistently, some patients with CVID have complications that might be related to T-cell deficiency, including opportunistic infections, autoimmune diseases, and malignancies, which is similar to that observed in patients with CID.[1,4] Therefore identifying novel markers to better classify CVID and distinguish CID from CVID will be required to best manage medical treatment for CVID.

We recently performed real-time PCR-based quantification of T-cell receptor excision circles (TREC) and signal joint immunoglobulin κ-deleting recombination excision circles (KREC) for mass screening of severe combined immunodeficiency (SCID)[5] and B-lymphocyte deficiency[6] in neonates. TREC and KREC are associated with T-cell and B-cell neogenesis, respectively.[7] Here we retrospectively report that TREC and KREC are useful for classifying patients with clinically diagnosed CVID.

Hypogammaglobulinemic patients (n = 113) were referred to our hospital for immunodeficiency from 2005-2011, and the following patients were excluded from the CVID pool by estimating their SCID genes based on clinical manifestations and lymphocyte subset analysis: 18 patients with SCID diagnoses; 14 patients less than 2 years of age (transient infantile hypogammaglobulinemia); 10 patients with IgM levels of greater than 100 mg/dL (hyper-IgM syndrome); 26 patients with diseases other than CVID caused by known gene alterations (10 with X-linked agammaglobulinemia and 11 with hyper-IgM syndrome